Received: 8 August 2022 | Revised: 12 October 2022 | Accepted: 14 October 2022

DOI: 10.1002/ardp.202200422

FULL PAPER

ARCH PHARM DPhG
Archiv der Pharmazie

New chimeric HDAC inhibitors for the treatment of colorectal cancer

Sofia I. Bär[1] | Rohan Pradhan[2] | Bernhard Biersack[1] | Bianca Nitzsche[3] | Michael Höpfner[3] | Rainer Schobert[1]

[1]Organic Chemistry Laboratory, University of Bayreuth, Bayreuth, Germany

[2]Care Group Sight Solution Pvt. Ltd., Dabhasa, Vadodara, India

[3]Institute of Physiology, Charité-Universitätsmedizin Berlin, Corporate member of Freie Universität Berlin, Humboldt-Universität zu Berlin and Berlin Institute of Health, Berlin, Germany

Correspondence
Sofia I. Bär, Organic Chemistry Laboratory, University of Bayreuth, Universitätsstraße 30, D-95447 Bayreuth, Germany.
Email: sofia.baer@uni-bayreuth.de

Abstract

Colorectal cancer is the third most common cause of cancer-associated deaths due to a high recurrence rate and an increasing occurrence of resistance to established therapies. This highlights the importance of developing new chemotherapeutic agents. The current study focuses on cancer-specific targets such as apoptosis-inhibiting survivin, which distinguishes cancer cells from healthy tissue. A combination of pharmacophores of established anticancer agents to afford chimeric pleiotropic chemotherapeutic agents was tested on this cancer entity. We analysed the effects of the dual mode anticancer agents, animthioxam, brimbam, troxbam, and troxham, as well as their structural congeners suberoylanilide hydroxamic acid and combretastatin A-4 on human cancer cell lines. Their cytotoxicity was determined using the MTT assay, further techniques for detecting apoptotic events, cell cycle analyses, clonogenic and wound healing assays, immunostaining, histone deacetylase (HDAC) activity measurements, and Western blot analysis for the detection of survivin expression in HCT116 colon cancer cells. Molecular docking studies were conducted to assess potential molecular targets of the test compounds. The test compounds were found selectively cytotoxic toward cancer cells by inducing apoptosis. The metastatic potential was effectively reduced by disruption of the microtubular cytoskeleton. The test compounds were also proven to be general HDAC inhibitors and to lead to reduced survivin expression.

KEYWORDS
chimeric compounds, colorectal cancer, histone deacetylase, hydroxamic acid, survivin

Abbreviations: CA-4, combretastatin A-4; HDAC, histone deacetylase; HDACi, HDAC inhibitor; IAP, inhibitor of apoptosis protein; LDH, lactate dehydrogenase; MTT, 3-(4,5-dimethylthiazol-2-yl)-2,5-diphenyltetrazolium bromide; SAHA, suberoylanilide hydroxamic acid.

1 | INTRODUCTION

Colorectal cancer is the third most common cause of new cases and deaths associated with cancer disease.[1] It features a high recurrence rate, not least because of aggressive medical procedures.[2] In addition, the frequency of occurrence of resistance against established drug regimens, for example, such employing 5-fluorouracil, is soaring for this cancer entity.[3] Hence, the quest for new treatment options needs to be intensified. One such new approach might be to identify cancer-only molecular modulators and targets for specially tailored new chemotherapeutic agents. The modulators of malignant tumors are as diverse as the disease itself. However, cancer cells share some common features, dubbed the hallmarks of cancer, that distinguish them from nonmalignant cells.[4–6] So far, these hallmarks comprise 14 central distinctive features, innate and acquired.[4,5] Histone deacetylase (HDAC) inhibitors (HDACis), show significant anticancer activity against leukemia as well as solid tumors, targeting the hallmark of replicative immortality through disruption of the DNA replication machinery.[4,5,7] The anticancer HDACi SAHA (vorinostat) is FDA approved for the treatment of patients with cutaneous T-cell lymphoma. Today, there are also numerous preclinical studies investigating the suitability of SAHA and other HDACi for the treatment of solid tumors, with promising results.[8,9] There are four classes of human HDAC enzymes containing a family of 18 members; class I comprises of HDACs 1–3 and 8, class II contains HDACs 4-7 as well as 9 and 10, class III members are called sirtuins and class IV comprises HDAC 11.[10,11] Each HDAC member displays different functions including deacetylation of histones as well as acting on non-histone substrates such as transcription factor p53 or cytoskeletal protein tubulin.[11] HDAC classes fall into two main groups as to their catalytic mechanisms. Classes I, II and IV are so called classical HDACs whose mechanisms of action are Zn^{2+} dependent, whereas class III sirtuins act NAD^{+} dependently.[11] SAHA inhibits class I and II HDACs at nanomolar concentrations.[11,12] A distinct downstream association of inhibition of HDAC 3 and 6 (members of class I and II HDACs) with a reduced survivin expression was reported.[13] This may be due to the inhibition of acetylation, where HDACs 3 and 6 specifically interact with survivin.[13] In particular, HDAC 6 which is present as a cytosolic protein, is known to control nuclear transport and thus the activity of survivin.[14,15] Survivin plays several roles regarding cell proliferation and survival as it improves the stability of microtubules, it is involved in cell cycle regulation, and as a member of the inhibitor of apoptosis proteins (IAP) it interferes with caspases 3 and 7. Further, it is nearly exclusively expressed in cancer cells and usually not expressed in most adult tissues, therefore it represents an interesting target for cancer therapy.[16–19] Since survivin is overexpressed in most cancer types, including colon, therapies inhibiting survivin expression might be highly cancer-specific, yet entity overarching.[16,20] Substances that target survivin have been of great interest in the last 20 years and there are several studies on survivin-related cancer treatments using small molecule inhibitors. Unfortunately, these studies failed due to various problems, such as too low selectivity, too high toxicity. An approach to circumvent these problems and to increase the effectiveness of the inhibitors is the use of hybrid substituents comprising a dual or synergistic mechanism of action.[21] Structural hybridization has already yielded several promising new anticancer compounds showing enhanced potency when compared to their individual structural constituents.[22] The structural motif "hydroxamic acid" is the central pharmacophore of HDACi SAHA and it is particularly easy to introduce into hybrid drugs.[23] In this work, a series of chimeric structures was synthesized by combining the crucial structural hydroxamic acid of SAHA with the *cis*-stilbene motif of the microtubule-destabilizing combretastatin A-4 (CA-4) (Figure 1). The resulting chimeric compounds were expected to have a pleiotropic mechanism of action and thus to achieve an optimization of action when compared to the lead compound SAHA. As a result of the dual attack with HDACi-mediated action and CA-4 mediated action, an enhanced or even synergistic effect can be expected, as has already been demonstrated for similar compounds.[24,25]

2 | RESULTS AND DISCUSSION

2.1 | Chemistry

The synthesis of the test compounds troxbam and troxham was described before (Scheme 1).[24] The new compound animthioxam was prepared from *t*-butyl 3-(5-formylthien-2-yl)acrylate **1** (obtained by Heck reaction of 5-bromo-2-formylthiophene with *t*-butyl acrylate), which underwent a van Leusen reaction with anisyl-TosMIC and methylamine leading to *t*-butyl cinnamate **2** in *t*-butanol (Scheme 1). Deprotection with TFA followed by reaction with THP-protected hydroxylamine led to compound **3**, which was converted to animthioxam upon treatment with 4 M HCl/dioxane in a methanolic solution. Brimbam was obtained in a similar way from

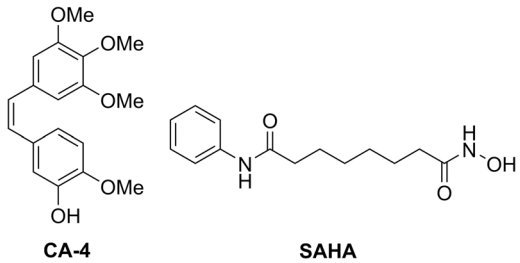

FIGURE 1 Lead structures of the chimeric compound series presented in this work. CA-4 is a microtubule polymerization inhibitor and SAHA an established HDACi. CA-4, combretastatin A-4; SAHA, suberoylanilide hydroxamic acid.

SCHEME 1 Syntheses and structures of hydroxamic acids used in this study. Reagents and conditions: (i) anisyl-TosMIC reagent, 33% $MeNH_2$/EtOH, K_2CO_3, *t*-BuOH, reflux, 2 h, 31%–79%; (ii) TFA, CH_2Cl_2, r.t., 1 h, then EDCI, DMAP, Et_3N, THPO-NH_2, CH_2Cl_2, r.t., 24 h, 57%–94%; (iii) 4 M HCl/dioxane, CH_2Cl_2/MeOH, r.t., 1 h, 81%–91%; (iv) 1 M NaOH, MeOH, r.t., 24 h, 100%; (v) *t*-BuOH, EDCI, DMAP, CH_2Cl_2, r.t., 24 h, 48%.

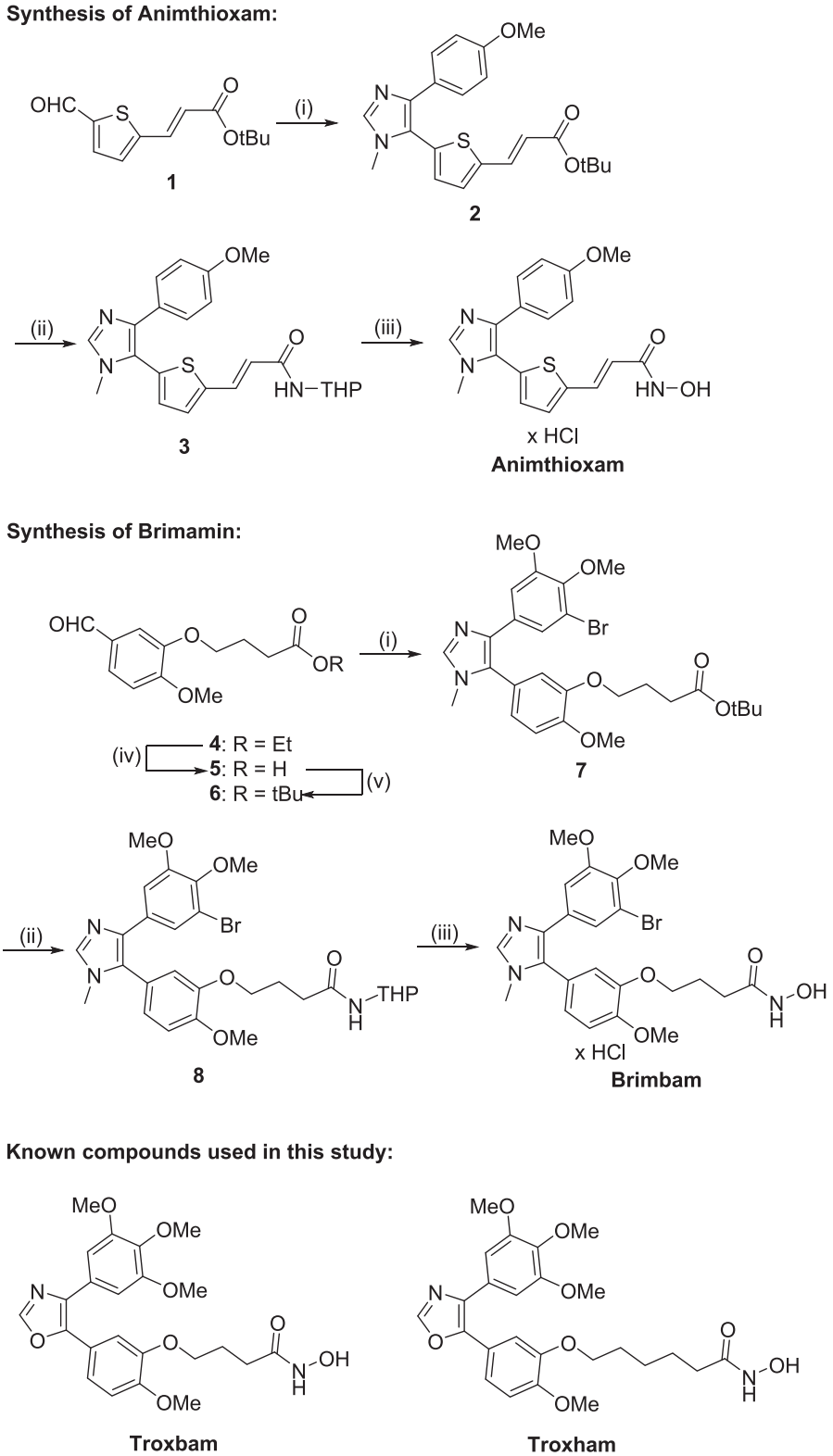

t-butyl ester **6**, which was obtained from ethyl-ester **4** followed by hydrolysis and esterification with *t*-butanol (Scheme 1).[24] Compound **6** was converted to imidazole **7** by reaction with 3-bromo-4,5-dimethoxyphenyl-TosMIC and methylamine. Removal of the *t*-butyl group by TFA afforded a carboxylic acid which was reacted with THP-protected hydroxylamine to give amide **8** which was deprotected with 4 M HCl/dioxane to furnish the target compound brimbam.

2.2 | Biological and biochemical evaluation

2.2.1 | Cytotoxicity toward cancer cells via the apoptotic pathway

Previously, some chimeric HDACi were reported to show distinct antiproliferative activity against cancer cells with IC_{50} values ranging from low µM to nM.[24,25] Troxbam and troxham already showed potent anticancer activity in earlier preliminary studies, which were not followed up on.[24] To ascertain the antiproliferative activity of the new chimeric HDACi candidates animthioxam and brimbam their IC_{50} values against several human cancer cell lines were assessed using MTT viability assays. Also, the IC_{50} values of the known analogues were completed to enable a meaningful comparison of their activities. Healthy cells (HDFa) were included in the cell line panel, and a selectivity index (SI) was calculated for each test compound. Table 1 summarizes the IC_{50} and SI values of the test compounds as well as of their structural congeners CA-4 and SAHA. All tested compounds exhibited IC_{50} values in the low µM to nM range whereas their cytotoxicity against the nonmalignant HDFa cells was low (≥50 µM). Troxbam stands out as the most active substance with the highest selectivity for cancer cells with an SI of >68.1. Regarding structure–activity relations, a longer linker (as in troxham vs. troxbam), or insertion of heteroatoms and changes of the trimethoxy motif (animthioxam and brimbam), appear to have a slightly negative effect on the antiproliferative activity.

In this study, the potential suitability of hybrid HDACi for the treatment of solid tumor entities was to be investigated. Since, on average, all test compounds were most active in colorectal cancer and comprise IC_{50} values in a similar concentration range, these cells were used for further experiments. Because many cancers lack a regulated induction of apoptosis, new potential anticancer drugs should be capable of inducing apoptotic cancer cell death.[26] The activities of effector caspases 3 and 7 are directly linked to activation of apoptosis pathways since they are key mediators of the mitochondrial apoptotic pathway.[27] To exclude necrosis playing a role in cancer cell death initiated by the new compounds, the lactate dehydrogenase (LDH) release by cancer cells upon compound treatment was measured.[28] As shown by fluorescent caspase 3/7 activity assays, all test compounds led to a significant induction of apoptosis when applied to colon cancer cells (Figure 2a), whereas no appreciable rise in LDH was detectable (Figure 2b). The induction of apoptosis in cancer cells is crucial for potential anticancer drugs since the suppression of apoptosis is one of those hallmarks of cancer, modulated by IAPs through direct inhibition of caspase 3/7.[29,30] The main cancer-specific IAP is called survivin, involved in several cancer-specific survival mechanisms and therefore comprising an interesting target for anticancer drugs.[17]

2.2.2 | Effects on the cell cycle progression of HCT116 colon carcinoma cells

To further elucidate the mechanism of action of our compounds, we analysed their effects on the progression of the cell cycle of $HCT116^{wt}$ colon carcinoma cells. Whereas all tested compounds led to a slight enhancement of the apoptotic cell fraction, only troxbam induced a distinct cell cycle arrest in the G2-M phase. This G2-M arrest is considerably more pronounced than that initiated by treatment with SAHA which is known to induce a G2-M arrest (Figure 3). A G2-M arrest is often associated with HDAC inhibition and induction of apoptosis by downregulation of the IAP survivin.[31,32]

2.2.3 | Metastatic potential and cellular dynamics

Virtually limitless cellular reproductive potential is one of the hallmarks of cancer. Therefore, we assessed the influence of our test compounds on this characteristic using the

TABLE 1 IC_{50} values (µM) of test compounds animthioxam, brimbam, troxbam, troxham as well as positive controls CA-4 and SAHA against the human cancer cell lines $HCT116^{wt}$ and its knockout mutant $HCT116^{p53}$ colon cancer, 518A2 melanoma, Huh7 and HepG2 liver cancer, as well as healthy human dermal fibroblasts (HDFa)

Compound	$HCT116^{wt}$	$HCT116^{p53-/-}$	518A2	Huh7	HepG2	HDFa	SI
Animthioxam	2.09 ± 0.45	1.42 ± 0.22	2.49 ± 0.28	3.53 ± 0.39	2.3 ± 0.2	>50	≥21.1
Brimbam	3.19 ± 0.21	1.9 ± 0.2	8.08 ± 0.92	9.27 ± 0.47	3.44 ± 0.80	>50	≥9.7
Troxbam	0.92 ± 0.12[a]	0.98 ± 0.03	0.64 ± 0.07[a]	0.95 ± 0.06[a]	0.18 ± 0.02[a]	>50	≥68.1
Troxham	0.61 ± 0.07[a]	0.8 ± 0.08	3.3 ± 0.3[a]	1.05 ± 0.04	3.4 ± 1	>50	≥27.3
CA-4	0.0026 ± 0.0002[a]	0.095 ± 0.03	0.018 ± 0.007[a]	0.045 ± 0.0041	0.0044 ± 0.00067	0.098 ± 0.0058	19.5
SAHA	0.9 ± 0.1[a]	1.10 ± 0.16	1.8 ± 0.1[a]	1.8 ± 0.5[b]	2.1 ± 0.4[b]	>50	≥32.5

Note: The selectivity index (SI) indicates the selectivity of the substances for cancer cells. Shown are the means ± standard deviation (SD) determined of four independent experiments. IC_{50} values were obtained by MTT assays from dose-response curves after 72 h incubation.

[a]Values obtained from Schmitt et al.[24]

[b]Values obtained from Bär et al.[25]

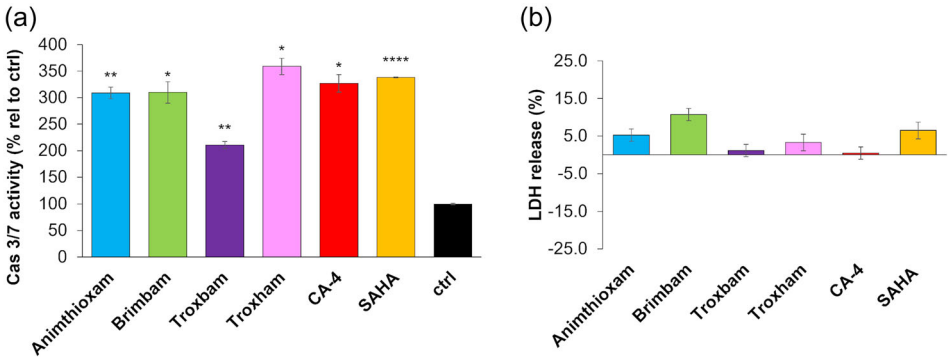

FIGURE 2 Results of the investigation of the type of cell death induced by treatment of the cells with the compounds. (a) Activation levels of effector caspases 3 and 7 in HCT116^{wt} cells after treatment with fourfold IC_{50} concentrations of compounds for 24 h. Corresponding concentration of DMSO was used as control (ctrl), set to 100%. Data shown represents means ± SD of four independent experiments, ****$p \le 0.001$; **$p \le 0.01$; *$p \le 0.05$, no sign means not significant. (b) LDH release of HCT116^{wt} cells after treatment with fourfold IC_{50} concentrations of compounds for 24 h. Corresponding concentration of DMSO was used as control (ctrl) which was set as 0% and maximum LDH release obtained by cell lysis was set as 100%. Data shown represents means ± SD of four independent experiments. CA-4, combretastatin A-4; DMSO, dimethyl sulfoxide; LDH, lactate dehydrogenase; SAHA, suberoylanilide hydroxamic acid.

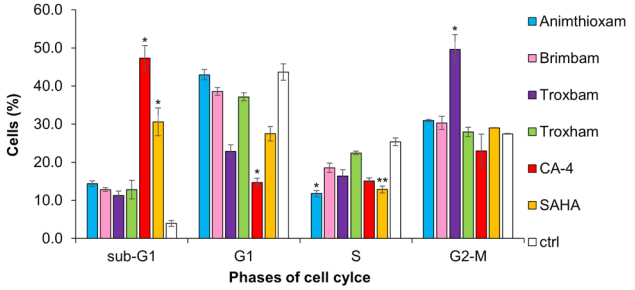

FIGURE 3 Distribution of HCT116^{wt} cells in different phases of the cell cycle measured by flow cytometry of PI stained cells. Cells were treated with IC_{50} of compounds for 24 h. Corresponding amounts of DMSO served as control (ctrl). Data represents the percentage of cells in each phase of the cell cycle as well as dead cells (sub-G1). Values represent means ± SD of three independent experiments. **$p \le 0.01$; *$p \le 0.05$, no sign means not significant. CA-4, combretastatin A-4; DMSO, dimethyl sulfoxide; SAHA, suberoylanilide hydroxamic acid.

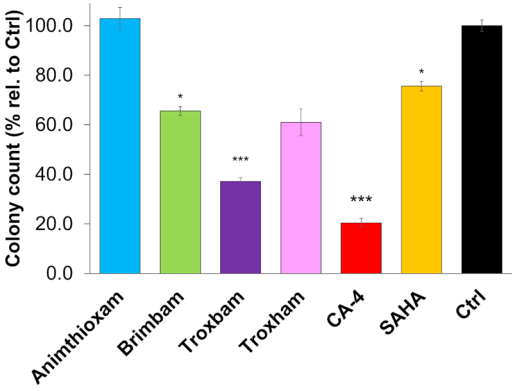

FIGURE 4 Colony count of HCT116^{wt} colon carcinoma cells obtained by colony formation assays after treatment of cells with IC_{50} of compounds for 24 h, respective concentration of DMSO served as control (Ctrl). The number of colonies is calculated as a percentage relative to the control which was set as 100%. Data shown represents means ± SD of three independent experiments, ***$p \le 0.005$; *$p \le 0.05$, no sign is equivalent to not significant. CA-4, combretastatin A-4; DMSO, dimethyl sulfoxide; SAHA, suberoylanilide hydroxamic acid.

clonogenic assay.[33,34] The clonogenic assay is used to assess the clonogenic potential of cells under the influence of test compounds or to assess the influence of other factors on the ability of single cells to form colonies. The clonogenic assay allows to measure and compare the percentage of cells that have the characteristic of being colony-forming.[34] As shown in Figure 4, the treatment of HCT116^{wt} colon carcinoma cells with IC_{50} concentrations of brimbam and troxbam resulted in a significant reduction of the clonogenic potential, whereas animthioxam and troxham did not significantly reduce the clonogenic potential. Both control substances CA-4 and SAHA induced a significant reduction of the clonogenic potential whereas the effect of CA-4 was clearly stronger and SAHA had only a weak effect. The effect induced by the test compounds brimbam and troxbam exceeded that of SAHA.

Taking into account the reduced clonogenic potential as well as the induction of potential HDACi-associated cell cycle arrests of colon carcinoma cells, we determined the influence of the test compounds on cellular migration using in vitro wound healing assays, monitoring the migration of the cells on a 2D surface. Brimbam and troxbam led to significant reductions in cellular migration when applied at IC_{50} concentration. Animthioxam and troxham did not attenuate the cellular motility much (Figure 5). While the effects of brimbam and troxbam were comparable to that of SAHA, CA-4 led to distinctly stronger retardation of cell migration.

To understand more precisely what the antimigratory effect is based on, we further observed the effect of test compounds on the

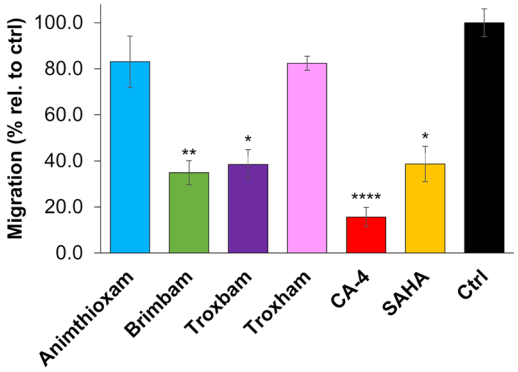

FIGURE 5 Cell migration of HCT116^{wt} colon carcinoma cells obtained by scratch migration assays under treatment of cells with IC_{50} of compounds for 24 h, respective concentration of DMSO served as control (Ctrl). Migration is calculated as a percentage relative to control which was set as 100%. Data shown represents means ± SD of three independent experiments, ****$p \le 0.001$; ***$p \le 0.005$; **$p \le 0.01$; *$p \le 0.05$, no sign is equivalent to not significant. CA-4, combretastatin A-4; DMSO, dimethyl sulfoxide; SAHA, suberoylanilide hydroxamic acid.

polymerization of purified tubulin monomers (Supporting Information: Figure 1). No inhibitory effect on tubulin polymerization could be observed for any of our test compounds, indicating a mode of action different to that of CA-4. HDACs mainly regulate the acetylation level of histones but also regulate the acetylation levels of nonhistone substrates such as tubulin.[35] HDACi like SAHA are known to act antimigratorily by inhibiting HDAC 6, which is a known key regulator of cytoskeleton dynamics, cell migration and cell–cell interactions.[35,36] As an effect of inhibiting these HDACs, the deacetylation of ac-α-tubulin is inhibited, which is resulting in altered cell dynamics as it disrupts the microtubule polymerization-depolymerization balance.[35] We immunostained the microtubule cytoskeleton of substance-treated cells to assess whether there are structural abnormalities associated with over-acetylation as a result of inhibited HDACs. The immunofluorescence images in Figure 6 reveal distinct structural changes of the microtubule skeleton upon treatment with active compounds. Brimbam and troxbam, in particular, led to clumpy-looking microtubules in colon cancer cells. The effect of CA-4 on the microtubules differs conspicuously, leading to a complete dissolution of the tubulin cytoskeleton.

2.2.4 | HDAC-associated mode of action

Results obtained so far clearly indicate an HDAC-associated mode of action for our test compounds. Based on this, their general HDAC inhibitory potential in HCT116 colon cancer cells was assessed using a commercial HDAC activity assay. The test compounds led to a reduction of general HDAC activity, with troxbam displaying the strongest effect, not much weaker than that of the clinically established HDACi SAHA (Figure 7a). Based on the demonstrated changes in tubulin dynamics, an association with inhibition of HDAC 6 is possible. Therefore, the most potent compound troxbam was investigated for its inhibitory effect on human HDAC 6. As shown in Figure 7b, concentration-dependent inhibition of HDAC 6 was obtained after troxbam treatment. The activity of HDAC 6 is almost halved by the addition of 1 µM troxbam, which corresponds to the IC_{50}. Therefore, it can be concluded that HDAC 6 inhibition is the key mechanism of action of this compound.

2.2.5 | Ac-α-tubulin levels and survivin expression levels

Taking into account the HDACi activity of our compounds, associated with apoptosis, and the cell cycle arresting effect of troxbam and alterations in microtubule cytoskeleton, we assumed HDAC 6 and downstream survivin to be very likely primary targets of them. As already mentioned by inhibition of HDAC 6, deacetylation of ac-α-tubulin is inhibited which results in reduced cellular dynamics.[35] Therefore, the expression levels of ac-α-tubulin and survivin in compound-treated colon cancer cells were assessed by means of western blot analysis. Troxbam and troxham led to significantly enhanced levels of ac-α-tubulin, while animthioxam and brimbam had no comparable effect. This is a further indication of HDAC 6 inhibition by the compounds troxbam and troxham, both comprising a stronger effect than SAHA. Troxbam and troxham also led to significantly reduced survivin expression levels, comparable to SAHA (Figure 8b). Survivin is a member of the IAP family and is involved in the regulation of the mitotoic spindle dynamics, the cell cycle, angiogenesis, and chemoresistance.[17] It is a desirable target of anticancer compounds since it is strongly expressed only in cancer cells where it acts as part of the survival machinery preventing induction of apoptosis.[17] Thus, the distinct downregulation of survivin by troxbam and troxham is a milestone of their preclinical evaluation as anticancer drug candidates.

2.3 | Molecular docking

HDAC6 is associated with the cell cycle and the cellular dynamics, as well as survivin, and therefore might be a central target of test compounds. Docking studies of test compounds bound to the catalytic center of human HDAC 6 (PDB ID 5EDU) were performed to determine their binding modes. The molecular docking was carried out with the Dockthor software in the presence of the catalytic Zn^{2+} ion at the binding site (Figure 9).

Except CA-4 all the compounds are forming bonds with the Zn. The Binding energies of all the molecules are more or less in the same region (−7 to −6 kcal) with animthioxam displaying the highest binding energy at −7.1 kcal (Table 2). Troxbam and troxham are forming hydrogen bonds with high number of amino acid residues and this maybe the reason for their relatively better biological activity. CA-4 is predominantly a tubulin inhibitor and does not seem to form a bond with Zn. But it is forming bonds with three amino acid

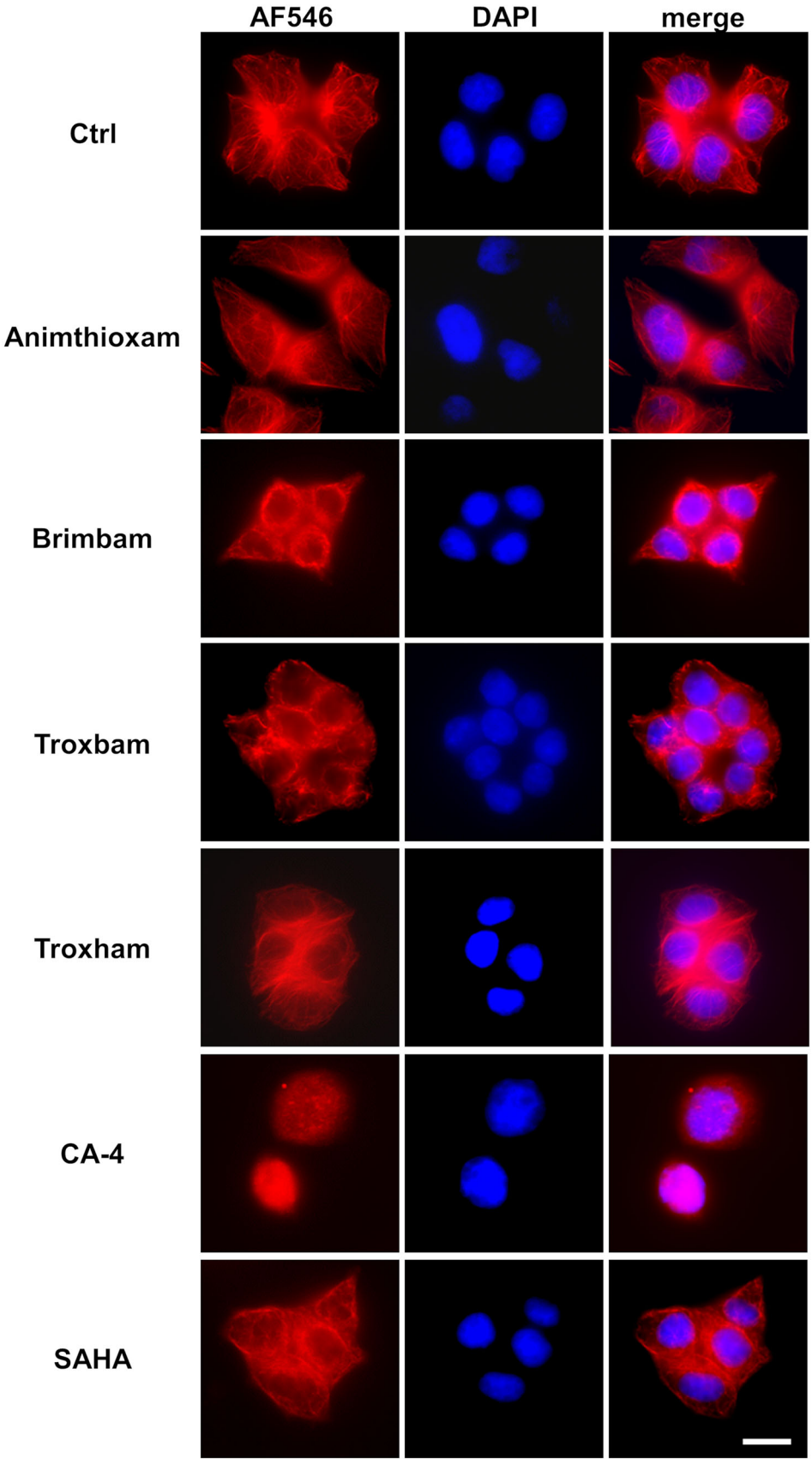

FIGURE 6 Immunofluorescence images of HCT116^{wt} cells, stained with anti-α-tubulin (AF546) and DAPI after treatment with IC_{50} concentrations of test compounds. Corresponding concentration of DMSO was used for treatment of control (Ctrl). Shown images are representative of at least three independent experiments. CA-4, combretastatin A-4; SAHA, suberoylanilide hydroxamic acid.

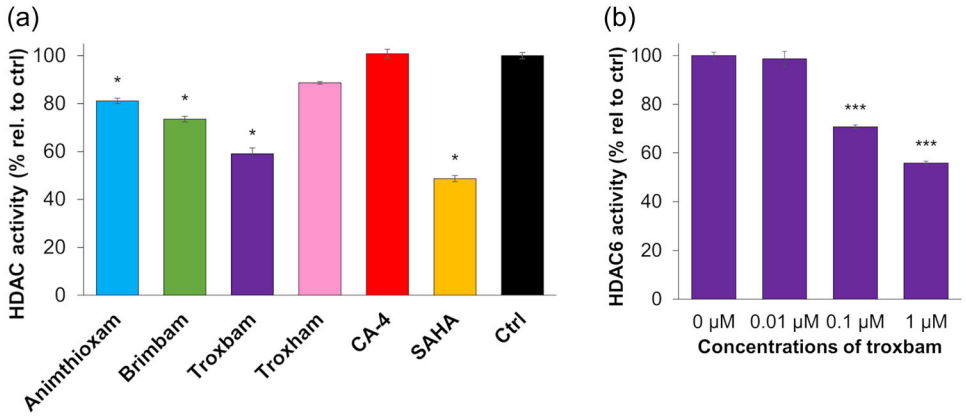

FIGURE 7 HDAC inhibitory activity of test compounds. (a) General HDAC activity of HCT116^{wt} cell lysate after treatment with IC_{50} concentrations of test compounds (animthioxam 2 µM, brimbam 3.2 µM, troxbam 0.9 µM, troxham 0.6 µM, and SAHA 0.9 µM). (b) Activity of human HDAC 6 after treatment with different concentrations of troxbam. Activities were normalized to Ctrl, respectively 0 µM, which was set to 100%. Data shown represent means ± SD of three independent experiments, $^{*}p \leq 0.05$; $^{***}p \leq 0.005$, no sign is equivalent to not significant. CA-4, combretastatin A-4; SAHA, suberoylanilide hydroxamic acid.

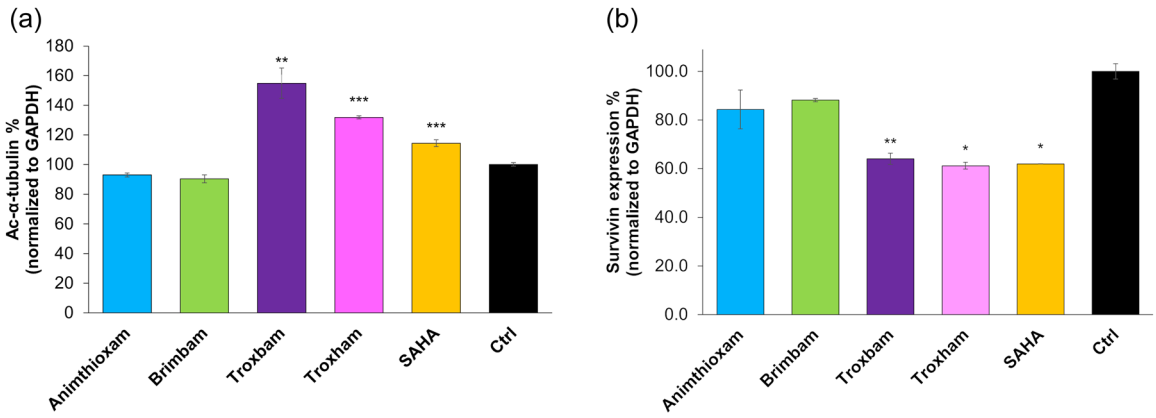

FIGURE 8 Levels of ac-α-tubulin and survivin in compound treated colon carcinoma cells. (a) Levels of ac-α-tubulin in HCT116 colon carcinoma cells, treated with corresponding IC_{50} concentrations of test compounds. (b) Survivin expression levels in HCT116 cells treated with IC_{50} concentrations of test compounds. Expression levels were normalized to GAPDH and relative to Ctrl which was set as 100%. Data shown represents means ± SD of three independent experiments, $^{*}p \leq 0.05$; $^{**}p \leq 0.01$; $^{***}p \leq 0.005$, no sign is equivalent to not significant.

residues (PHE565, THR563, and SER453) in the pocket. However, the amino acids with which it is forming bonds are quite different from the ones formed by our ligands. This difference maybe one of the reasons for the vastly different biological activities displayed by CA-4 and the compounds designed by us.

3 | CONCLUSION

Two new chimeric Z-stilbene–hydroxamate conjugates, animthioxam and brimbam, were modeled on the monomodal drugs CA-4 and SAHA. Unlike the latter, they showed multimodal, pleiotropic effects in a series of assays for anticancer activities. They were tested alongside their known structural congeners troxbam and troxham, as well as CA-4 and SAHA. Except for brimbam, all chimeric conjugates tested showed a higher selectivity for cancer cells than CA-4. Troxbam was particularly impressive with a cancer selectivity exceeding that of the established HDACi SAHA. Moreover, the cell cycle inhibitory effect of troxbam on colon carcinoma cells in G2-M phase was exceptional and significantly stronger than the effect elicited by SAHA. Troxbam also outperformed SAHA when it comes to the antimigratory effect and HDAC inhibition. Generally, HDAC 6 inhibition appears to be the main mechanism of action of the chimeric test compounds, an assumption also supported by molecular docking studies. In particular, HDAC 6 is associated with cell dynamics, and expression levels of the apoptosis inhibiting and cell cycle regulating protein survivin. In addition

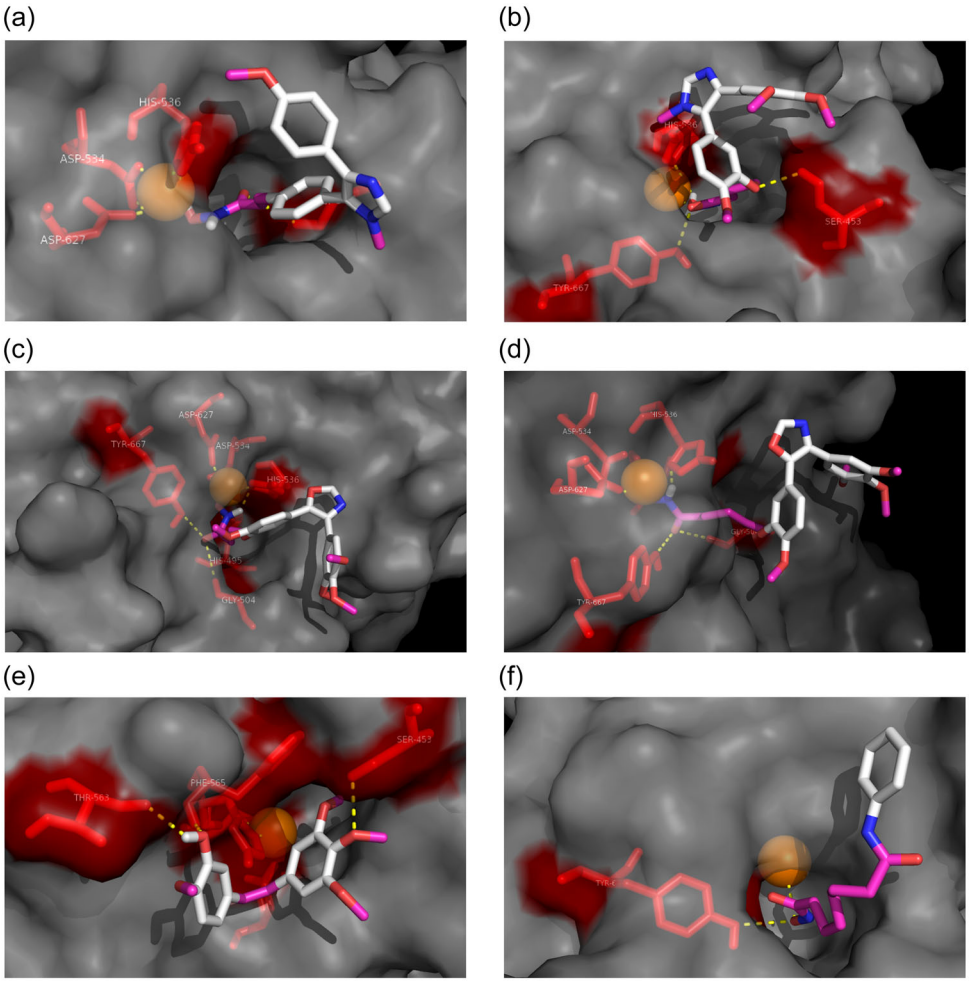

FIGURE 9 Molecular docking poses on class II HDAC6 using Docthor software. Docking images of (a) animthioxam, (b) brimbam, (c) troxbam, (d) troxham, (e) combretastatin A-4, and (f) suberoylanilide hydroxamic acid.

TABLE 2 Calculated binding energies (BE) with 5EDU of test compounds animthioxam, brimbam, troxbam, troxham, SAHA, and CA-4 using AutoDock-Vina 1.1.2 software

Compound	BE (kcal/mol)	Residues	Bond with Zn
Animthioxam	−7.1	GLY504, ASP627, HIS536, ASP534,	Yes
Brimbam	−6.5	SER453, HIS536, TYR667	Yes
Troxbam	−6.4	ASP534, HIS536, ASP627, HIS495, TYR667, GLY504	Yes
Troxham	−6.6	ASP534, GLY504, HIS495, ASP627, HIS536, TYR667	Yes
CA-4	−5.9	PHE565, THR563, SER453	No
SAHA[a]	−6.2	TYR667	Yes

to the HDAC 6 inhibitory effect, associated hyperacetylation of alpha-tubulin and decreased expression of survivin were detected upon compounds treatment of colon carcinoma cells. The observed downregulation of the cancer-specific protein survivin by troxbam and troxham adds to the multimodal and cancer-specific character of this new structural motif, recommending them for a further assessment of their suitability as chemotherapeutic agents. The results obtained in this study contribute to consider the suitability of hybrid HDACi for the treatment of solid tumors. As HDACi have so far only been approved for the treatment of leukemic disease, this raises the prospect of a new field of application for structurally related hybrid compounds.

4 | EXPERIMENTAL

4.1 | Chemistry

4.1.1 | General remarks

All starting compounds and reagents were purchased from the usual retailers and used without further purification. Column chromatography: silica gel 60 (230-400 mesh). Melting points (uncorrected), Electrothermal 9100; NMR spectra (see the Supporting Information), Bruker Avance 300 spectrometer; chemical shifts are given in parts per million (δ) downfield from tetramethylsilane as internal standard; Mass spectra, Thermo Finnigan MAT 8500 (EI), UPLC/Orbitrap (ESI-HRMS). Elemental analysis were carried out with an Elementar UNICUBE (Elementar Analysensysteme GmbH).

4.1.2 | Synthesis of animthioxam

*1-Methyl-4-(4-methoxyphenyl)-5-(4′-tert.-butoxycarbonylethenyl-thienyl)imidazole (**2**)*

A mixture of 4-formyl-tert.-butyl-2-thienylacrylate **1** (100 mg, 0.42 mmol) and 33% $MeNH_2$/ethanol (260 µl, 2.10 mmol) in *t*-butanol (15 ml) was refluxed for 2 h. After cooling to room temperature, anisyl-tosylmethylisocyanide (126 mg, 0.42 mmol) and K_2CO_3 (500 mg, 3.62 mmol) were added and the reaction mixture was refluxed for 4 h. The solvent was evaporated, the residue diluted with ethyl-acetate, washed with water and brine, dried over Na_2SO_4, filtered, and concentrated in vacuum. The residue was purified by column chromatography (silica gel 60, ethyl-acetate/methanol 9:1). Yield: 50 mg (0.13 mmol, 31%); R_f = 0.72 (ethyl-acetate/methanol, 9:1); yellow oil; ν_{max} (ATR)/cm^{-1} 2968, 2936, 2901, 2837, 1699, 1623, 1526, 1504, 1454, 1389, 1368, 1292, 1207, 1144, 1104, 1029, 968, 921, 833, 798, 743, 706, and 640; ^{1}H-NMR (300 MHz, $CDCl_3$) δ 1.49 (9H, s), 3.54 (3H, s), 3.76 (3H, s), 6.13 (1H, d, *J* = 15.6 Hz), 6.79 (2H, d, *J* = 9.0 Hz), 6.95 (1H, d, *J* = 3.7 Hz), 7.19 (1H, d, *J* = 3.7 Hz), 7.46 (2H, d, *J* = 9.0 Hz), 7.60 (1H, s), 7.63 (1H, d, *J* = 15.6 Hz); ^{13}C-NMR (75.5 MHz, $CDCl_3$) δ 28.2, 32.3, 55.1, 80.7, 113.7, 119.8, 126.6, 127.8, 128.0, 128.1, 129.9, 130.5, 130.8, 133.3, 135.5, 138.4, 141.2, 142.0, 158.7, and 165.8; *m/z* (%) 396 (37) [M$^+$], 340 (100), 57 (20).

*1-Methyl-4-(4-methoxyphenyl)-5-(4′-tetrahydropyranyloxyaminocarbonylethenyl-thienyl)imidazole (**3**)*

Compound **2** (79 mg, 0.20 mmol) was dissolved in CH_2Cl_2 (3 ml), treated with TFA (2 ml) and stirred at room temperature for 1 h. The solvent was evaporated, the residue was dried in vacuum and used for the next step without further purification. It was dissolved in dry CH_2Cl_2 and EDCI (101 mg, 0.52 mmol), DMAP (19 mg, 0.15 mmol), triethyl-amine (120 µl, 0.57 mmol), and tetrahydropyranyl-hydroxylamine (73 mg, 0.63 mmol) were added. After stirring at room temperature for 24 h, the solvent was evaporated and the residue was purified by column chromatography (silica gel 60, ethyl-acetate/methanol, 9:1). Yield: 50 mg (0.11 mmol, 57%), R_f = 0.56 (ethyl-acetate/methanol, 9:1); ν_{max} (ATR)/cm^{-1} 3167, 2949, 2872, 1659, 1615, 1526, 1504, 1454, 1389, 1347, 1292, 1246, 1204, 1175, 1133, 1113, 1031, 966, 947, 924, 895, 873, 834, 812, and 728; ^{1}H-NMR (300 MHz, $CDCl_3$) δ 1.58–1.96 (6H, m), 3.46 (3H, s), 3.62–3.74 (1H, m), 3.73 (3H, s), 4.05–4.10 (1H, m), 5.00–5.07 (1H, m), 5.98–6.12 (1H, m), 6.75 (2H, d, *J* = 9.0 Hz), 6.89 (1H, d, *J* = 3.7 Hz), 7.12–7.14 (1H, m), 7.47 (2H, d, *J* = 9.0 Hz), 7.58 (1H, s), 7.70–7.77 (1H, m); ^{13}C-NMR (75.5 MHz, $CDCl_3$) δ 14.1, 18.5, 21.0, 24.8, 25.0, 25.6, 28.0, 32.2, 55.1, 60.3, 62.3, 67.9, 102.5, 113.7, 117.4, 119.8, 126.2, 128.0, 130.6, 130.8, 131.0, 132.3, 138.3, 140.8, 142.8, 158.8, and 171.1; *m/z* (%) 439 (26) [M$^+$], 355 (100), 339 (88), 296 (37), 243 (34), 165 (21), 85 (56), and 41 (34).

1-Methyl-4-(4-methoxyphenyl)-5-(4′-hydroxyaminocarbonylethenylthienyl)-imidazole × HCl (animthioxam)

Compound **3** (50 mg, 0.11 mmol) was dissolved in CH_2Cl_2/MeOH (5 ml, 4:1) and 4 M HCl/dioxane (3 ml) was added. The reaction mixture was stirred at room temperature for 1 h. The solvent was evaporated and the residue was crystallized from ethanol/*n*-hexane. Yield: 35 mg (0.089 mmol, 81%); yellow solid of mp 178–180°C; ν_{max} (ATR)/cm^{-1} 3122, 3007, 2969, 2840, 2539, 1647, 1599, 1575, 1558, 1536, 1511, 1462, 1422, 1399, 1357, 1335, 1296, 1250, 1224, 1210, 1182, 1107, 1050, 1023, 1003, 962, 920, 852, 815, 798, 720, 709, and 689; ^{1}H-NMR (300 MHz, DMSO-d_6) δ 3.72 (3H, s), 3.77 (3H, s), 6.26 (1H, d, *J* = 15.6 Hz), 7.02 (2H, d, *J* = 8.8 Hz), 7.41–7.45 (3H, m), 7.52 (1H, d, *J* = 3.8 Hz), 7.63 (2H, d, *J* = 8.8 Hz), 9.23 (1H, s), 10.70–10.92 (1H, br s); ^{13}C-NMR (75.5 MHz, DMSO-d_6) δ 33.9, 55.3, 114.5, 119.3, 119.8, 121.3, 126.2, 129.0, 130.5, 131.0, 132.1, 133.3, 136.6, 143.7, 160.0, and 161.9; *m/z* (%) 355 (18) [M$^+$], 340 (100), 311 (88), 44 (77); Elemental analysis, Anal. calcd. for $C_{18}H_{18}ClN_3O_3S$: C, 55.17; H, 4.63; N, 10.72. Found: C, 55.30; H, 4.68; N, 10.64.

4.1.3 | Synthesis of brimbam

*5-Formyl-2-methoxyphenyloxybutyric acid (**5**)*

Ethyl-5-formyl-2-methoxyphenyloxybutyrate **4** (120 mg, 0.42 mmol) was dissolved in MeOH (10 ml), aqueous NaOH (1 M, 10 ml) was added and the reaction mixture was stirred at room temperature for 24 h. The solution was acidified with aqueous HCl (1 M, to pH < 2) and extracted with ethyl-acetate. The organic phase was dried over Na_2SO_4 and concentrated in vacuum. Yield: 99 mg (0.42 mmol, 100%); colorless solid of mp 127–128°C; ν_{max} (ATR)/cm^{-1} 3025, 2974, 2922, 2708, 2625, 1708, 1682, 1581, 1509, 1472, 1439, 1410, 1397, 1361, 1341, 1295, 1263, 1243, 1213, 1184, 1161, 1137, 1088, 1061, 1029, 1015, 931, 883, 858, 818, 796, 769, 750, 680, and 641; ^{1}H-NMR (300 MHz, $CDCl_3$) δ 2.15–2.19 (2H, m), 2.59 (2H, t, *J* = 7.2 Hz), 3.91 (3H, s), 4.11 (2H, *t*, *J* = 6.2 Hz), 6.95 (1H, d, *J* = 8.2 Hz), 7.38 (1H, s), 7.44 (1H, d, 8.2 Hz), 9.91 (1H, s); ^{13}C-NMR (75.5 MHz, $CDCl_3$) δ 24.1, 30.4, 56.1, 67.7, 110.7, 126.9, 130.0, 148.8, 154.9, 178.7, and 191.0; *m/z* (%) 238 (57) [M$^+$], 221 (4), 151

(100), 137 (14), 123 (22), 109 (16), 95 (13), 87 (38), 77 (13), and 43 (25).

*tert.-Butyl 5-formyl-2-methoxyphenyloxybutyrate (**6**)*

Compound **5** (99 mg, 0.42 mmol), DMAP (25 mg, 0.21 mmol) and tert.-butanol (45 µl, 0.48 mmol) were dissolved in CH_2Cl_2 (5 ml) and EDCI (88 mg, 0.46 mmol) was added. The reaction mixture was stirred at 0°C for 2 h and then at room temperature for 24 h. The reaction solution was purified by column chromatography. Yield: 60 mg (0.20 mmol, 48%); R_f = 0.76 (ethyl-acetate/*n*-hexane, 1:1); ν_{max} (ATR)/cm^{-1} 2977, 2935, 2843, 1724, 1684, 1595, 1585, 1509, 1436, 1392, 1367, 1339, 1322, 1263, 1239, 1151, 1133, 1020, 960, 922, 865, 846, 808, 778, 747, 734, and 640; ^{1}H-NMR (300 MHz, $CDCl_3$) δ 1.43 (9H, s), 2.18–2.26 (2H, m), 2.43 (2H, t, J = 7.4 Hz), 3.93 (3H, s), 4.09 (2H, t, J = 6.4 Hz), 6.95 (1H, d, J = 8.2 Hz), 7.39 (1H, s), 7.43–7.47 (1H, m), 9.82 (1H, s); ^{13}C-NMR (75.5 MHz, $CDCl_3$) δ 24.6, 28.1, 32.0, 56.1, 68.1, 80.4, 110.7, 110.9, 126.6, 130.1, 149.0, 154.9, 172.3, and 190.9; *m/z* (%) 294 (15) [M^+], 221 (86), 152 (100), 143 (23), 87 (96), 69 (34), 57 (45), and 41 (19).

*1-Methyl-4-(3-bromo-4,5-dimethoxyphenyl)-5-(4'-methoxy-3'-tert.-butoxycarbonylpropylphenyl)-imidazole (**7**)*

Compound **6** (141 mg, 0.48 mmol) was dissolved in tert.-butanol (10 ml) and 33% $MeNH_2$/EtOH (297 µl, 2.4 mmol) was added. The reaction mixture was stirred under reflux for 1 h. (3-Bromo-4,5-dimethoxyphenyl)-tosylmethylisocyanide (175 mg, 0.48 mmol) and K_2CO_3 (500 mg, 3.62 mmol) were added and the reaction mixture was stirred under reflux for 2 h. The solvent was evaporated, the residue was taken up in ethyl-ester and washed with water. The organic phase was dried over Na_2SO_4, filtered and the filtrate was concentrated in vacuum. The residue was purified by column chromatography (silica gel 60). Yield: 213 mg (0.38 mmol, 79%); R_f = 0.63 (ethyl-acetate); ν_{max} (ATR)/cm^{-1} 2978, 2936, 2836, 1726, 1599, 1584, 1547, 1510, 1484, 1464, 1416, 1392, 1368, 1320, 1247, 1151, 1137, 111, 1042, 1026, 1000, 947, 890, 865, 808, 759, 737, 680, 659, 638, and 619; ^{1}H-NMR (300 MHz, DMSO-d_6) δ 1.37 (9H, s), 1.88–1.93 (2H, m), 2.31–2.35 (2H, m), 3.44 (3H, s), 3.56 (3H, s), 3.67 (3H, s), 3.82 (3H, s), 3.91–3.96 (2H, m), 6.90–6.97 (2H, m), 7.05–7.16 (2H, m), 7.22 (1H, s), 7.75 (1H, s); ^{13}C-NMR (75.5 MHz, DMSO-d_6) δ 24.3, 27.7, 31.2, 31.7, 55.4, 55.6, 60.0, 67.6, 79.6, 109.5, 112.5, 115.6, 116.4, 120.9, 122.1, 123.5, 128.9, 132.5, 134.7, 137.7, 143.6, 148.1, 149.6, 152.8, and 171.7; *m/z* (%) 562 (100) [M^+], 560 (98) [M^+], 506 (23), 504 (22), 491 (25), 489 (43), 487 (22), 420 (41), 418 (45), 405 (15), 403 (16), 87 (23), 57 (17).

*1-Methyl-4-(3-bromo-4,5-dimethoxyphenyl)-5-(4'-methoxy-3'-tetrahydropyranyloxyaminocarbonyl-propylphenyl)-imidazole (**8**)*

Compound **7** (202 mg, 0.36 mmol) was dissolved in CH_2Cl_2 (3 ml), treated with TFA (2 ml) and stirred at room temperature for 1 h. The solvent was evaporated, the residue was dried in vacuum and used for the next step without further purification. It was dissolved in dry CH_2Cl_2 and EDCI (108 mg, 0.56 mmol), DMAP (21 mg, 0.15 mmol), triethyl-amine (130 µl, 0.61 mmol) and tetrahydropyranyl-hydroxylamine (78 mg, 0.67 mmol) were added. After stirring at room temperature for 24 h, the solvent was evaporated and the residue was purified by column chromatography (silica gel 60, ethyl-acetate/methanol, 9:1). Yield: 205 mg (0.34 mmol, 94%), R_f = 0.44 (ethyl-acetate/methanol, 9:1); ν_{max} (ATR)/cm^{-1} 2946, 2877, 2841, 1674, 1600, 1548, 1512, 1487, 1465, 1417, 1320, 1249, 1205, 1172, 1135, 1113, 1040, 1022, 1001, 947, 897, 868, 801, 760, 725, 680, 659, 645, 618, and 604; ^{1}H-NMR (300 MHz, $CDCl_3$) δ 1.52–1.61 (3H, m), 1.76–1.84 (3H, m), 2.08–2.13 (2H, m), 2.29–2.38 (2H, m), 3.44 (3H, s), 3.50–3.58 (1H, m), 3.64 (3H, s), 3.88–3.90 (4H, m), 3.98 (2H, *t*, J = 6.1 Hz), 4.90–4.94 (1H, m), 6.81 (1H, s), 6.81–6.96 (2H, m), 7.06 (1H, s), 7.22 (1H, s), 7.50 (1H, s), 8.95–9.02 (1H, br s); ^{13}C-NMR (75.5 MHz, $CDCl_3$) δ 18.7, 24.7, 25.0, 28.0, 29.8, 32.1, 55.7, 56.0, 60.5, 62.5, 68.2, 102.4, 109.8, 112.1, 116.0, 17.3, 122.3, 122.5, 122.8, 123.9, 128.9, 131.9, 136.3, 137.1, 144.7, 148.5, 150.1, 153.2, and 170.1; *m/z* (%) 605 (2) [M^+], 603 (2) [M^+], 561 (3), 559 (4), 521 (3), 519 (3), 505 (6), 503 (7), 477 (100), 475 (97), 420 (59), 418 (62), 405 (38), 403 (39), 380 (63), 85 (27), and 44 (49).

1-Methyl-4-(3-bromo-4,5-dimethoxyphenyl)-5-(4'-methoxy-3'-hydroxyaminocarbonylpropylphenyl)-imidazole × HCl (brimbam)

Compound **8** (205 mg, 0.34 mmol) was dissolved in CH_2Cl_2/MeOH (5 ml, 4:1) and 4 M HCl/dioxane (3 ml) was added. The reaction mixture was stirred at room temperature for 1 h. The solvent was evaporated and the residue was crystallized from ethanol/*n*-hexane. Yield: 175 mg (0.31 mmol, 91%); colorless solid of mp 157–158°C; ν_{max}(ATR)/cm^{-1} 3350, 3060, 3014, 2947, 2876, 2837, 1732, 1638, 1547, 1524, 1494, 1459, 1418, 1398, 1342, 1311, 1260, 1247, 1215, 1182, 1139, 1114, 1042, 1019, 994, 947, 888, 853, 809, 758, 739, 724, 676, 639, 620; ^{1}H NMR (300 MHz, DMSO-d_6) δ 1.85–1.98 (2H, m), 2.09–2.17 (2H, m), 3.58 (3H, s), 3.63 (3H, s), 3.72 (3H, s), 3.84 (3H, s), 3.93–3.97 (2H, m), 7.05–7.07 (1H, m), 7.15–7.26 (4H, m), 9.33 (1H, s), 10.50–10.57 (1H, br s); ^{13}C-NMR (75.5 MHz, DMSO-d_6) δ 24.6, 28.6, 33.8, 55.7, 56.1, 60.2, 68.0, 111.3, 112.6, 115.4, 116.8, 117.6, 122.3, 124.0, 127.6, 130.1, 135.5, 145.9, 148.4, 150.7, 153.2, 168.5; *m/z* (%) 520 (94) [M^+], 518 (93) [M^+], 505 (25), 503 (25), 477 (14), 475 (14), 420 (16), 418 (15), 405 (11), 403 (12), 101 (100), 59 (24), 36 (54); HRMS for $C_{23}H_{27}O_6N_3{}^{79}Br$ [M^++H] calcd. 520.10777, found 520.10688, for $C_{23}H_{27}O_6N_3{}^{81}Br$ [M^++H] calcd. 522.10573, found 522.10464.

4.1.4 | Synthesis of troxbam and troxham

Troxbam and troxham were obtained according to the literature.[24]

4.2 | Biological assays

4.2.1 | Stock solutions

Compounds were dissolved in DMSO to obtain a concentration of 10 mM and stored at −23°C. Before biological experiments, they

were diluted to the desired concentration with sterile Millipore water. CA-4 and SAHA were purchased from TCI chemicals.

4.2.2 | Cell lines and cell culture conditions

518A2 human melanoma cells (Department of Radiotherapy & Radiobiology, University Hospital Vienna, Austria), HCT116^{wt} (DSMZ ACC-581) and its HCT116$^{p53-/-}$ knockout mutant colon carcinoma cells, Huh7 (CVCL_0336) and HepG2 (DSMZ ACC-180) liver carcinoma as well as HDFa human dermal fibroblasts (ATCC PCS-201-012) as healthy control cell line were cultivated in Dulbeccos Modified Eagle medium (DMEM, PAN biotech), supplemented with 10% (v/v) fetal bovine serum (Sigma Aldrich) and 1% (v/v) ZellShield (Minerva Biolabs) at 37°C under 95% humidity and 5% CO_2. If not noted otherwise, all bioassay steps including cells were conducted under these standard cell culture conditions.

4.2.3 | MTT cell viability assay

The antiproliferative effect of test compounds on cancer cell lines as well as on human dermal fibroblasts was examined using the 3-(4,5-dimethylthiazol-2-yl)-2,5-diphenyltetrazolium bromide (MTT) based cell viability assay. The MTT cell viability assay was conducted as described before.[37] Briefly, cells were seeded in 96-well microtiter plates (Sarstedt) with a cell density of 0.05×10^6 cells per ml with 100 µl per well and incubated for 24 h under standard cell culture conditions. Afterwards, a dilution series of test compounds was added, followed by a further incubation step for 72 h. A 0.05% in MTT in PBS solution was added (12.5 µl/well), followed by another incubation period of 2 h. Following a centrifugation step, the medium was discarded and 25 µl per well of SDS solution in DMSO (10% SDS, 0.6% AcOH in DMSO) were added, and plates were further incubated for 1 h. Absorbance was measured at 570 nm and 630 nm using a Tecan Plate reader. Background absorbance (630 nm) was subtracted from formazan signal (570 nm). Resulting absorbance is directly proportional to viable cells, control was normalized to 100% viable cells and accordingly the viability of cells treated with test compounds was calculated. IC_{50} was calculated based on a sigmoidal fit model using GraphPad Prism. Means and SD were calculated from at least four independent experiments.

4.2.4 | Caspase 3/7 assay

Activation of caspases 3 and 7 is strongly associated with induction of apoptotic type of cell death. Levels of active caspase 3/7 in HCT116^{wt} cells were measured using a commercial caspase 3/7 activity apoptosis assay kit (green fluorescence, CellMeter™, AAT Bioquest, catalog number 22796). The protocol was in accordance with the procedure specified by the manufacturer. Briefly, the cells were seeded into a black 96-well plate as well as into a clear 96-well plate for the corresponding MTT assay. After treatment with test compounds for 24 h, the caspase 3/7 working solution was added, followed by further incubation in the dark at room temperature for 1 h. Fluorescence intensity was monitored at ex/em = 485/535 nm using a Tecan plate reader.

4.2.5 | LDH release assay[28]

HCT116^{wt} colon carcinoma cells were seeded in 96 well flat bottom microtiter plates (Sarstedt) with 100 µl per well and a cell density of 0.05×10^6 cells per ml, wells containing medium alone were additionally set for background measurement. Cells were allowed to grow overnight under standard cell culture conditions followed by substance treatment with 11.1 µl of 10-fold concentrated test compound dilutions for 24 h. For maximum LDH release 10 µl per well of lysis solution (9% Triton-X100 in Millipore H_2O) were added and incubated for 45 min, same amount was added to maximum release background correction wells containing only medium. After centrifugation (4°C, 150*g*, 5 min) 50 µl of the supernatant of each well were transferred on a fresh microtiter plate followed by addition of 50 µl LDH assay buffer (223 mg 2-*p*-iodophenyl-3-*p*-nitrophenyl-5-phenyl-tetrazolium-chloride, 57 mg *N*-methylphenazonium-methyl-sulfate, 575 mg *N*-adenine-dinucleotide, 3.2 g lactic acid in 480 ml 200 mM Tris-Cl, pH 8.0) per well. Plate was incubated in the dark for 10–30 min at room temperature. Then 50 µl stop solution (1 M acetic acid) were added per well and absorbance was measured at 490 nm. Mean value of background wells was subtracted from negative control and test wells as well as maximum LDH release wells. Afterwards percentage of LDH release was calculated, setting maximum LDH release as 100%. Means and SD were calculated from at least three independent experiments.

4.2.6 | Cell cycle distribution

The distribution of HCT116 colon carcinoma cells in the different phases of the cell cycle under influence of test compounds was analyzed using flow cytometry as recently described.[38] Briefly, cells were seeded in 6-well microtiter plates (Sarstedt) and allowed to grow for 24 h, followed by treatment with test compounds to obtain final concentrations corresponding the IC_{50} and further incubation period of 24 h. Afterward, medium and cells of each well were transferred into precooled centrifugation tubes (on ice) and centrifuged (300 g, 5 min, 4°C). The pellet was resuspended with 1 ml ice-cold EtOH (70%) and cells were fixed for at least 1 h at 4°C. Cellular DNA was stained with 200 µl propidium iodide solution (50 µg/ml PI, 0.1% sodium citrate, 50 µg/ml RNase A, freshly added in PBS) for 40 min at 37°C and 500 µl PBS were added per sample. Cell cycle distribution of cells was obtained using flow cytometry and analyzed by CXP analysis software (Beckman Coulter). Means ± SD of $n = 3$.

4.2.7 | Clonogenic assay[33]

The clonogenic assay also known as colony formation assay monitors the ability of single cancer cells to grow into a colony. To monitor influence of test compounds on this ability, HCT116 colon carcinoma cells were treated with compounds before the assay. After 24 h of treatment, cells were rinsed with PBS and harvested using trypsination. Afterwards, 500 cells per well were seeded into 6-well plates (Sarstedt), containing 3 ml DMEM and incubated for 7 days under regular medium change. After the growth period, medium was discarded, and wells were carefully rinsed with PBS followed by fixation of colonies by adding 1 ml EtOH absolute (VWR) per well for 3 min. Colonies were stained for 5 min using 1 ml per well of a 0.5% crystal violet solution, then wells were rinsed with water. Resulting stained colonies were counted using imageJ (Vs 1.53j, National Institutes of Health). Colony count was normalized to control which was set as 100%.

4.2.8 | Scratch migration assay[39]

The scratch migration assay also known as wound healing assay is an easy and cheap method for investigating cell migration in vitro. For the assay, HCT116wt colon cancer cells were seeded in wells of a 24-well microtiter plate (Sarstedt) in 500 µl DMEM containing 10% (v/v) FBS (Sigma Aldrich) and 1% (v/v) ZellShield (Minerva Biolabs) with a density of 0.5×10^6 cells per ml. When cells reached a confluent level, medium was changed to DMEM containing 0.1% FBS followed by further incubation overnight. The following day, a 10 µl pipette tip was used to scratch a wound into the cell monolayer. Afterward, each well was rinsed with PBS to remove detached cells and 1 ml per well of fresh DMEM containing 0.1% FBS was added. Substance treatment ensued by adding 10.1 µl per well of 100-fold test compound dilutions. Images of scratch areas were acquired using inverted brightfield microscopy. Cells were further incubated, and images of the same areas were acquired after 6 and 24 h. The course of migration of the cells into the area of the artificially created wound was evaluated using ImageJ (vs. 1.53j, National Institutes of Health). Cellular migration capability was calculated relative to control which was set as 100%.

4.2.9 | Tubulin polymerization assay

To monitor the effect of test compounds on the polymerization of tubulin monomers a tubulin polymerization assay was conducted. Before the assay 10-fold predilutions of test compounds were prepared in Brinkley's Buffer (BRB80; 80 mM PIPES KOH, 1 mM $MgCl_2$, 1 mM EGTA). A volume of 11.1 µl of substance predilution were added per well containing 50 µl 2× polymerization buffer (20% glycerin, 3 mM GTP in BRB80, sterile) into a flat black 96-well plate (Brand). Then, 50 µl of purified pork brain tubulin (10 mg/ml) were added in each well, obtaining a final concentration of 10 µM of test compounds. The corresponding dilution of DMSO served as control (ctrl). Tubulin polymerization at 37°C was measured via OD340 nm using a TECAN plate reader.

4.2.10 | Immunofluorescence staining

To visualize the effects of test compounds on the morphology of the α-tubulin cytoskeleton of HCT116 colon cancer cells, immunofluorescence staining was conducted as described before.[38] Briefly HCT116^{wt} colon cancer cells were seeded onto cover slips (borosilicate glass, Carl Roth) inside the wells of 24-well microtiter plates and allowed to grow for 24 h. Followed by compound treatment with concentrations corresponding the IC_{50} of test compounds for 24 h, whereas corresponding amount of DMSO served as control (ctrl). Before immunofluorescence staining cells were fixed using a 3.7% formaldehyde solution in PBS. Immunofluorescence staining of α-tubulin, as well as DAPI counterstaining, were conducted. The condition of the α-tubulin cytoskeleton was documented by fluorescence microscopy.

4.2.11 | HDAC activity assays

For measuring the HDAC activity of HCT116^{wt} colon cancer cells under the influence of test compounds, a commercial fluorometric HDAC activity kit was used (Amplite™, Fluorimetric HDAC Activity Assay Kit, green fluorescence, AAT Bioquest, Catalog number: 13601). Before the assay, a cell lysate was prepared from HCT116^{wt} colon cancer cells. The assay was conducted as described by the provider. Briefly, a fivefold dilution of HCT16^{wt} cell lysate in assay buffer was treated for 15 min at 37°C with different concentrations of prediluted test compounds (final concentrations corresponding the IC_{50}; animthioxam 2 µM, brimbam 3.2 µM, troxbam 0.9 µM, troxham 0.6 µM and SAHA 0.9 µM). After adding HDAC Green™ Substrate working solution, an incubation step followed (room temperature, 30–60 min, in the dark). Fluorescence was measured at ex/em = 490/525 nm using a TECAN plate reader.

For measuring HDAC 6 activity of human HDAC 6, a commercial fluorometric HDAC 6 activity kit (BioVision, HDAC 6 Activity Assay Kit [Fluorometric], Catalog Number K466). The assay was conducted as described by the provider. Briefly, a dilution of 2 µl of human HDAC 6 in 0.5 ml of HDAC 6 assay buffer was used. Samples were treated for 15 min at 37°C with different concentrations of prediluted troxbam (final concentrations 0.01, 0.1, and 1 µM). After adding HDAC 6 Substrate working solution, an incubation step followed (37°C, 30 min, in the dark). Developers were added and samples were further incubated for 10 min at 37°C, afterwards, fluorescence was measured at ex/em = 380/490 nm in an end point mode at 37°C.

4.2.12 | Western blot

Western blots were conducted following a standard protocol.[40] Briefly, cells were seeded into six-well plates (0.15×10^6 cells per well) and allowed to grow overnight. The following day cells were treated with desired concentrations of test compounds. After further incubation for 24–72 h, cells were lysed to obtain whole cell lysate and amount of protein was determined using Pierce™ BCA Protein Assay Kit (Catalog Number 23225). Protein samples were mixed with 4× Lämmli buffer (Biorad, Catalog Number 1610747) and denatured for 5 min at 95°C. A total amount of 30 µg protein per sample was applied to a precast 12% polyacryl amide Mini-PROTEAN gel (Biorad) and electrophoresis was conducted. Afterward, proteins were electroblotted onto a 0.2 µm PVDF membrane (ROTI®PVDF, CarlRoth). After blocking for 1 h in 5% skimmed milk solution, primary antibody incubation (anti-GAPDH, 1:1000, CellSignaling, Catalog Number 5174; anti-survivin, 1:1000, CellSignaling, Catalog Number 2808, anti-ac-α-tubulin 1:1000, Merck Catalog-Number T7451) followed over night at 4°C. Following day membranes were washed in 0.1% Tween in TBS and incubated with secondary HRP-conjugated antibody (anti-rabbit 1:2000, CellSignaling, Catalog Number 7074, anti-mouse 1:2000, CellSignaling, Catalog Number 7076) for 1 h at room temperature. Protein signals were obtained using Clarity Max Western ECL Substrate (Biorad, Catalog Number 1705062) and captured using ChemiDoc system (Biorad). For quantification, ImageJ (vs. 1.53j, National Institutes of Health) was used and the density of the protein bands was normalized to GAPDH as a loading control.

4.3 | Statistics

Statistical data analysis was performed using DATAtab Team (2022) Online Statistics Calculator.DATAtab e.U. Graz, Austria. URL https://datatab.net. If not indicated otherwise, the presented data is the mean ± SD. To test statistical significance one-way analysis of variance coupled with Tukey's post hoc tests was used. Several replicates of each experiment were carried out, the exact number is given in the respective figure or table description.

4.4 | Molecular docking

Docking studies of test compounds on the active site of human HDAC6 (PDB ID 5EDU) were carried out using AutoDock Vina in the presence of the catalytic Zn^{2+} ion at the binding site. The cocrystallized ligands and the Zn^{2+} ion were used as reference to define the binding pockets within a radius of 30 Å. The protein preparation and ligand preparation procedures were done using the open-source web server Dockthor (www.dockthor.lncc.br, accessed on October 19, 2021) and Merck molecular force field was applied. The protein preparation was done at physiological pH 7.4. All dockings and calculations were performed using AutoDock-Vina 1.1.2 software.[41] All other settings for ligand and receptor definitions were used as defaults. The docking strategy, scoring, and chemical parameters were kept as default. For each compound, nine poses were generated, and all were evaluated with the built-in scoring function. PyMOL software is utilized to visualize, compare and analyze binding pose predictions, and to create images.[42] For visualization, the protein was used in the cartoon mode and the surface mode, wherein the metal chelation of Zn^{2+} was visualized in the sphere mode and nb sphere mode. The binding energies do have some variability of 1–2 kcal. The development of computational methods for protein flexibility is still in its infancy and thereby remains one of the major future directions in protein-ligand docking which will increase its accuracy.

ACKNOWLEDGMENT

Open Access funding enabled and organized by Projekt DEAL.

CONFLICTS OF INTEREST

The authors declare no conflicts of interest.

ORCID

Sofia I. Bär http://orcid.org/0000-0002-8612-3516
Bernhard Biersack http://orcid.org/0000-0001-7305-346X
Rainer Schobert http://orcid.org/0000-0002-8413-4342

REFERENCES

[1] R. L. Siegel, K. D. Miller, H. E. Fuchs, A. Jemal, *CA Cancer J. Clin.* **2022**, *72*, 7. https://doi.org/10.3322/caac.21708
[2] Z. Liu, T. Lu, J. Li, L. Wang, K. Xu, Q. Dang, C. Guo, L. Liu, D. Jiao, Z. Sun, X. Han, *Cancer Cell. Int.* **2021**, *21*, 359. https://doi.org/10.1186/s12935-021-02070-z
[3] W. A. Hammond, A. Swaika, K. Mody, *Ther. Adv. Med. Oncol.* **2016**, *8*, 57. https://doi.org/10.1177/1758834015614530
[4] D. Hanahan, R. A. Weinberg, *Cell* **2011**, *144*, 646. https://doi.org/10.1016/j.cell.2011.02.013
[5] D. Hanahan, *Cancer Discov.* **2022**, *12*, 31. https://doi.org/10.1158/2159-8290.CD-21-1059
[6] D. Hanahan, R. A. Weinberg, *Cell* **2000**, *100*, 57. https://doi.org/10.1016/S0092-8674(00)81683-9
[7] P. A. Marks, R. Breslow, *Nat. Biotechnol.* **2007**, *25*, 84. https://doi.org/10.1038/nbt1272
[8] A. C. West, R. W. Johnstone, *J. Clin. Invest.* **2014**, *124*, 30. https://doi.org/10.1172/JCI69738
[9] B. Biersack, B. Nitzsche, M. Höpfner, *Cancer Drug Resist.* **2022**, *4*, 64. https://doi.org/10.20517/cdr.2021.105
[10] M. I. Y. Elmallah, O. Micheau, *Cancers* **2019**, *11*, 850. https://doi.org/10.3390/cancers11060850
[11] I. Gregoretti, Y.-M. Lee, H. V. Goodson, *J. Mol. Biol.* **2004**, *338*, 17. https://doi.org/10.1016/j.jmb.2004.02.006
[12] W. K. Kelly, P. A. Marks, *Nat. Clin. Pract. Oncol.* **2005**, *2*, 150. https://doi.org/10.1038/ncponc0106
[13] J. Y.-C. Lee, C.-W. Kuo, S.-L. Tsai, S. M. Cheng, S.-H. Chen, H.-H. Chan, C.-H. Lin, K.-Y. Lin, C.-F. Li, J. R. Kanwar, E. Y. Leung, C. C. H. Cheung, W.-J. Huang, Y.-C. Wang, C. H. A. Cheung, *Front. Pharmacol.* **2016**, *7*, 81. https://doi.org/10.3389/fphar.2016.00081
[14] S. Kaur, P. Rajoria, M. Chopra, *Cell. Oncol.* **2022**, *45*, 779. https://doi.org/10.1007/s13402-022-00704-6
[15] M. T. Riolo, Z. A. Cooper, M. P. Holloway, Y. Cheng, C. Bianchi, E. Yakirevich, L. Ma, Y. E. Chin, R. A. Altura, *J. Biol. Chem.* **2012**, *287*, 10885. https://doi.org/10.1074/jbc.m111.308791

[16] K. Roy, N. Singh, R. K. Kanwar, J. R. Kanwar, *Recent Pat. Anticancer Drug Discov.* **2016**, *11*, 152. https://doi.org/10.2174/1574892811666160229121815
[17] A. C. Mita, M. M. Mita, S. T. Nawrocki, F. J. Giles, *Clin. Cancer Res.* **2008**, *14*, 5000. https://doi.org/10.1158/1078-0432.CCR-08-0746
[18] D. C. Altieri, *Cancer Lett.* **2013**, *332*, 225. https://doi.org/10.1016/j.canlet.2012.03.005
[19] D. C. Altieri, *Nat. Rev. Cancer* **2003**, *3*, 46. https://doi.org/10.1038/nrc968
[20] P. J. Kim, J. Plescia, H. Clevers, E. R. Fearon, D. C. Altieri, *Lancet* **2003**, *362*, 205. https://doi.org/10.1016/s0140-6736(03)13910-4
[21] Y. Li, W. Lu, J. Yang, M. Edwards, S. Jiang, *Expert Opin. Biol. Ther.* **2021**, *21*, 1429. https://doi.org/10.1080/14712598.2021.1918672
[22] A. Shalini, V. Kumar, *Expert Opin. Drug Discov.* **2021**, *16*, 335. https://doi.org/10.1080/17460441.2021.1850686
[23] B. Biersack, S. Polat, M. Höpfner, *Semin. Cancer Biol.* **2022**, *83*, 472. https://doi.org/10.1016/j.semcancer.2020.11.005
[24] F. Schmitt, L. Gosch, A. Dittmer, M. Rothemund, T. Mueller, R. Schobert, B. Biersack, A. Volkamer, M. Höpfner, *Int. J. Mol. Sci.* **2019**, *20*, 383. https://doi.org/10.3390/ijms20020383
[25] S. Bär, A. Dittmer, B. Nitzsche, G. Ter-Avetisyan, M. Fähling, A. Klefenz, L. Kaps, B. Biersack, R. Schobert, M. Höpfner, *Int. J. Oncol.* **2022**, *60*, 73. https://doi.org/10.3892/ijo.2022.5363
[26] S. W. Fesik, *Nat. Rev. Cancer* **2005**, *5*, 876. https://doi.org/10.1038/nrc1736
[27] S. A. Lakhani, A. Masud, K. Kuida, G. A. Porter, C. J. Booth, W. Z. Mehal, I. Inayat, R. A. Flavell, *Science* **2006**, *311*, 847. https://doi.org/10.1126/science.1115035
[28] F. K.-M. Chan, K. Moriwaki, M. J. de Rosa, *Methods Mol. Biol.* **2013**, *979*, 65. https://doi.org/10.1007/978-1-62703-290-2_7
[29] E. C. LaCasse, S. Baird, R. G. Korneluk, A. E. MacKenzie, *Oncogene* **1998**, *17*, 3247. https://doi.org/10.1038/sj.onc.1202569
[30] A. M. Hunter, E. C. LaCasse, R. G. Korneluk, *Apoptosis* **2007**, *12*, 1543. https://doi.org/10.1007/s10495-007-0087-3
[31] S. Zhu, Y. Li, L. Zhao, P. Hou, C. Shangguan, R. Yao, W. Zhang, Y. Zhang, J. Tan, B. Huang, J. Lu, *J. Cell. Biochem.* **2012**, *113*, 2375. https://doi.org/10.1002/jcb.24109
[32] W. Feng, D. Cai, B. Zhang, G. Lou, X. Zou, *Biomed. Pharmacother.* **2015**, *74*, 257. https://doi.org/10.1016/j.biopha.2015.08.017
[33] N. A. P. Franken, H. M. Rodermond, J. Stap, J. Haveman, C. van Bree, *Nat. Protoc.* **2006**, *1*, 2315. https://doi.org/10.1038/nprot.2006.339
[34] M. Kurt Yüksel, P. Topçuoğlu, M. Kurdal, O. Ilhan, *Cytotherapy* **2010**, *12*, 38. https://doi.org/10.3109/14653240903313958
[35] J. Schemies, W. Sippl, M. Jung, *Cancer Lett.* **2009**, *280*, 222. https://doi.org/10.1016/j.canlet.2009.01.040
[36] A. Valenzuela-Fernández, J. R. Cabrero, J. M. Serrador, F. Sánchez-Madrid, *Trends Cell Biol.* **2008**, *18*, 291. https://doi.org/10.1016/j.tcb.2008.04.003
[37] S. I. Bär, M. Gold, S. W. Schleser, T. Rehm, A. Bär, L. Köhler, L. R. Carnell, B. Biersack, R. Schobert, *Chemistry—A European Journal* **2021**, *27*, 5003. https://doi.org/10.1002/chem.202005451
[38] M. Rothemund, S. I. Bär, T. Rehm, H. Kostrhunova, V. Brabec, R. Schobert, *Dalton Trans.* **2020**, *49*, 8901. https://doi.org/10.1039/d0dt01664k
[39] C.-C. Liang, A. Y. Park, J.-L. Guan, *Nat. Protoc.* **2007**, *2*, 329. https://doi.org/10.1038/nprot.2007.30
[40] T. Mahmood, P.-C. Yang, *N. Am. J. Med. Sci.* **2012**, *4*, 429. https://doi.org/10.4103/1947-2714.100998
[41] O. Trott, A. J. Olson, *J. Comput. Chem.* **2009**, *31*, NA. https://doi.org/10.1002/jcc.21334
[42] W. DeLano, *CCP4 Newsl. Protein Crystallogr.* **2002**, *44*, 1.

SUPPORTING INFORMATION

Additional supporting information can be found online in the Supporting Information section at the end of this article.

How to cite this article: S. I. Bär, R. Pradhan, B. Biersack, B. Nitzsche, M. Höpfner, R. Schobert, *Arch. Pharm.* **2023**;356:e2200422. https://doi.org/10.1002/ardp.202200422